A REVIEW ON LASER MACHINING OF ALUMUNIA CERAMIC

B. Umroh[1,2], Md Nizam Abd Rahman[1,*], Mohd Najib Ali Mokhtar[1], A. Ginting[3], Irianto[4], R.L. Muhamud[5], and Hidayatulah Himawan[6]

Received: March 28, 2023; Revised: May 19, 2023; Accepted: May 20, 2023

Abstract

Alumina, renowned for its outstanding resistance to corrosion and heat, poses a formidable challenge due to its brittle nature when it comes to machining. Nonetheless, laser machining has emerged as a particularly suitable method for working with hard and brittle materials like alumina. While traditional machining techniques can also be effective, they often necessitate prolonged machining durations and significantly high tool wear rates, thereby driving up the overall machining costs. By employing experimentation and optimization techniques, laser machining technologies such as Nd: YAG lasers, fiber lasers, and CO_2 lasers have displayed remarkable efficacy in machining alumina. Notably, CO_2 lasers offer distinctive advantages owing to their maximum power output of 45 kW and laser wavelength of 10.6 µm, rendering them suitable for macro material cutting applications. This paper aims to consolidate pertinent information on laser machining of alumina into a single document. The primary focus of this paper revolves around key laser machining parameters, including pulse duration, frequency, peak power, laser power, piercing time, gas pressure, and cutting speed, along with their impact on machining quality aspects such as surface irregularity, kerf width, taper angle, and the Heat-Affected Zone (HAZ).

Keywords: **Alumina; Laser Machining; Machining Parameters; Quality Geometry; Structural damage**

[1] *Faculty of Manufacturing Engineering, Universiti Teknikal Malaysia Melaka, Jalan Hang Tuah Jaya, 76100 Durian Tunggal, Melaka, Malaysia. E-mail: mdnizam@utem.edu.my[*]; najibali@utem.edu.my*

[2] *Department of Mechanical Engineering, Faculty of Engineering Universitas Medan Area, Jalan Kolam No. 1, 20223 Medan Estate, Indonesia. E-mail: bobbyumroh@staff.uma.ac.id*

[3] *Laboratory of Machining Processes, Department of Mechanical Engineering, Faculty of Engineering, Universitas Sumatera Utara, Jalan Almamater, Building J17.01.01, Medan 20155, Indonesia. E-mail: armansyah.ginting@usu.ac.id*

[4] *Department General Education, Faculty of Resilience, Rabdan Academy, Abu Dhabi, United Arab Emirates. E-mail: iharny@ra.ac.ae*

[5] *RS Advanced Technology Sdn. Bhd. No. 35G, Jalan Mutiara Subang 1, Taman Mutiara Subang, 47500 Subang Jaya, Selangor, Malaysia. E-mail: Maju_saintifik98@yahoo.com*

[6] *Universitas Pembangunan Nasional Veteran Yogyakarta, Indonesia. E-mail: if.iwan@upnyk.ac.id*

[*] *Corresponding Author*

DOI:

Suranaree J. Sci. Technol. 30(3):010233(1-13)

Introduction

Alumina is a type of white ceramic that is used extensively in industry as an insulator, abrasion-resistant plates, and resistor washers. Simply put, alumina is an inorganic crystalline substance that falls within the category of non-metallic materials (Samant and Dahotre, 2008; Ruys, 2019). Alumina has superior thermal stability over metals and plastics and they are as solid as metals and rarely undergo chemical reactions (Rakshit and Das, 2019). Because of its many useful properties, ceramic alumina is widely used in producing vehicles, airplanes, electronics, medical equipment, and other items that must maintain a constant temperature (Li *et al*., 2017; Carvalho *et al*., 2018, 2020; Pappas *et al*., 2020).

Alumina can be effectively processed through abrasive machining, which is considered a precise method for material removal (Tuersley *et al*., 1994; Shen *et al*., 2002). However, extensive research by Black and Chua (1997) revealed that this approach is time-consuming and leads to notable increases in manufacturing expenses. Furthermore, conventional machining operations involving ceramic materials tend to cause rapid wear of cutting tools due to the physical contact between the tool and the workpiece and the vibration generated by the rotating spindle (Abdullah *et al*., 2013, 2015; Sarkar *et al*., 2017; Marimuthu *et al*., 2019b).

The laser ablation process provides an alternative method for machining alumina, effectively addressing concerns related to tool wear and machining time. This process stands out due to its non-contact material removal and high vaporization rate capabilities (Sharma *et al*., 2020; You *et al*., 2020)

Achieving precision in laser drilling and cutting operations is a crucial factor for the success of the overall laser machining process. The effect of parameter settings on surface quality, metallurgical properties, machined workpiece geometry, and material removal rate has been extensively studied in the context of laser beam machining (LBM) (Gautam and Pandey, 2018a). This report examines and analyzes published research on the use of Nd: YAG laser, fiber laser, and CO_2 laser machining processes on alumina ceramics.

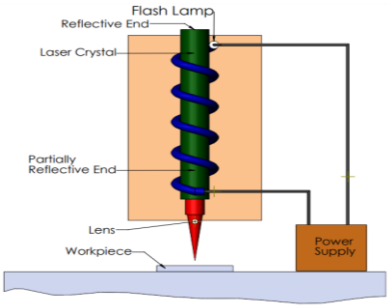

Figure 1.The Schematic of Laser Beam Machining

Laser Beam Machining Process

LBM is a heating process carried out by using laser light which produces high heat energy generated by a laser beam focused on a single point that can remove some matter through the process (Tanaka *et al*., 2019; Bhattacharyya and Doloi, 2020). One difference between laser machining and mechanical processing is that it is easily controlled by a Computer Numeric Control (CNC) LBM capable of covering small areas and large sizes (Nagimova and Perveen, 2019). Furthermore, the laser beam machining process can melt the material by ablation through high temperatures, resulting in precision cutting (Wen *et al*., 2019). The schematic diagram of laser beam machining is shown in Figure 1. An equation can be found in laser machining with temperature distribution closely related to surface quality, so a method could be found to simulate the determination of the heat load (Fu *et al*., 2015) as follows.

$$I = \frac{AP}{\pi r_0^2} \exp\left[-B\left(\frac{r}{r_0}\right)^2\right] \quad (1)$$

Where I is the intensity of the laser, P is the power of the laser, A is the absorption coefficient of the laser, r_0 is the radius of the point, B is the coefficient of the Gaussian distributed heat flux, and r is the distance to the center beam. Alternatively, the radius of the laser beam can be calculated using the equation (Salonitis *et al*., 2007) below:

$$r = r_0\left[1 + \left(M^2 \frac{\lambda(z+\delta f}{\pi r_0^2}\right)^2\right]^{1/2} \quad (2)$$

where r is the laser beam radius at a depth z from the work piece surface, M is the beam quality parameter, λ the laser wavelength, and δf is the position of the focal plane relative to the work piece surface. In principle the material is liquefied during the on-position time of each pulse, where energy will be lost because the conduction from the molten pool to the material does not melt around it so that the energy entering the material can be calculated by the equation (Salonitis *et al*., 2007):

$$Q_{in} = Q_L + Q_{cond} + Q_{conv} \quad (3)$$

where Qin is the energy that enters the work piece in a pulse from the laser beam, Q_L the energy consumed for phase change, Q_{cond} the heat conducted in the workpiece, and Q_{conv} is the heat lost by convection to air.

Nd: YAG Laser

Nd: YAG (Yttrium Neodymium-Doped Aluminum Garnet; Nd: $Y_3Al_5O_{12}$) and CO_2 lasers are the two most used hole-making laser systems. Nd: YAG cannot tolerate higher energy densities, so it cannot be utilized for long-term measurements. For cutting complicated geometries in general and reflective sheet materials in particular, Nd: YAG laser machining is considered the most suitable cutting tool (Harimkar and Dahotre, 2009; Gautam and Pandey, 2018b). Several investigators have carried out Nd: YAG laser ceramic machining with parameters such as laser power, pulse repetition rate, pulse width, and rotating speed that have been shown to boost efficiency, productivity, and precision; with accurate size and final quality (Mohammed *et al*., 2019). The most typical emission wavelength of Nd: YAG is 1064 µm, as stated by (Arshad *et al*., 2020). In pulse mode, the Nd: YAG laser offers high peak power in a short time, hence boosting thermal impact and allowing for the drilling of thick materials with outstanding focusing capabilities appropriate for drilling with various materials. Figure 2. is a schematic of the Nd: YAG laser.

Fiber Laser

Fiber lasers are part of laser beam processing. Fiber lasers are typically in high demand in the industry due to their excellent beam quality, high energy efficiency, reasonable cost, compact size, and high-speed processing (Marimuthu *et al*., 2019a). Most fiber lasers use the Q switch operating mode. However, the advent of the "main oscillator, power amplifier" (MOPA) design allows for width-independent control, pulse, and frequency pulse repetition rate for fiber laser specifications which have been presented in Table 1. below:

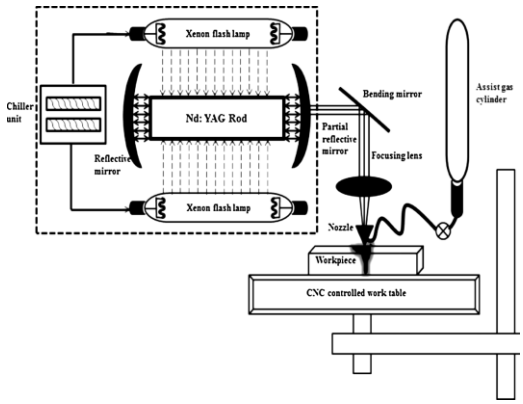

Figure 2. Schematic diagram of a Nd: YAG laser (Gautam and Pandey, 2018)

Fiber lasers are widely used to process materials such as titanium, stainless steel and magnesium alloys (Parmar *et al*., 2019). Previous researchers (Yan, Li, Sezer, Whitehead, *et al*., 2011b) have successfully cut a 6mm thick alumina sheet with a fiber laser, where high laser peak power (1 kW), short pulse duration (5 ms), and pulse repetition rate (30 Hz) resulted in a cut with no crack on alumina material. Furthermore, (Marimuthu, Dunleavey and Smith, 2019b) explains that high gas pressure can produce a higher quality surface finish where the heat-affected area is low, the oxide layer is thin and uniform, and there is less heat visible area.

CO_2 Laser

The CO_2 laser is an electric gas release process that uses three gases, namely carbon dioxide (25%) as the active medium, nitrogen (10-55%) as the fill medium, and helium (40-88%) as the medium fill. The CO_2 laser operates in the infrared region, 10.6 µm. Laser light amplification occurs in an optical resonator consisting of two cavity mirrors, such as a fully reflecting concave mirror and a partially transmitting output mirror. The output power of the carbon dioxide laser beam ranges from 10W to 45kW. CO_2 lasers can be obtained in continuous waveform (CW) and pulse wave (PW). The peak power for the PW CO_2 laser is very high, even if the average power is low. CO_2 lasers can produce output with 10-15% conversion efficiency. Due to the high atmospheric pressure operated by the CO_2 laser, the process is prevalent because it is very versatile and has high power. Therefore, it is widely used in industry for cutting, assembly, and surface engineering (Oosterbeek *et al*., 2016; Yilbas *et al*., 2016).

Table 1. Fiber laser specifications (Bhattacharyya and Doloi, 2020)

Machine model	Description
Laser Wavelength	1.064µm
Mode of operation	Pulsed
Mode of the laser beam	TEM
Beam diameter	8.8-9mm
Laser beam spot diameter	18-20µm (after focus)
Pulse repetition rate	50-120kHz
Output fiber length	3m

Studies on alumina machining have been performed using a CO_2 Laser, specifically parts >4 mm thick. Machining is done by changing some parameters and using a power of 1.8-3.5 KW mm, and according to the research, the results of the CO_2 laser have shown good performance (Yan *et al*., 2011a; Bharatish *et al*., 2015). However, CO_2 lasers are commonly used in industry for cutting due to their high power, with light emitted at wavelengths that are safer for the eyes (Rakshit and Das, 2019). The technical specifications of the CO_2 laser are shown in Table 2.

Laser Machining of Alumina Ceramic

As previously explained, this alumina, with the introduction of Al_2O_3, is a reliable material in its application. Liquid alumina forms at 2327 K and is stable up to 3500K. At temperatures above 3250K, the ceramic splits to produce different substances such as AlO(g), Al(l), Al(g), Al_2O(g), and AlO_2(g). At temperatures above 5000K, complete separation and oxygen atoms and alumina vapor are formed (Gautam and Pandey, 2018b) (Samant and Dahotre, 2009). From several theories, laser machining of alumina can be done with equation 1 because of the combination of melting, dissociation, and evaporation.

$$Al_2O_3 = 2Al\ (l) + 3/2\ O_2\ (g) \quad (4)$$

During alumina laser machining, the most important thing to do is to minimize surface roughness and machining damage. Many researchers have conducted optimization and modeling studies related to laser machining with some parameters, but so far, many parameters are possible for controlling the quality of the object. However, thermal properties are also the primary basis for the ability of alumina (Furukawa *et al*., 1956). In this review, we will look at issues related to surface roughness and damage of alumina.

Surface Roughness

Laser beam machining efficiency depends on the process and material parameters, where one of the material parameters is Ra (surface roughness) (Khed, 2015). The machining quality is also determined by the surface roughness required for the application (Dubey and Yadava, 2008) . Researchers have previously reported that CO_2 laser machining has surface roughness values strongly influenced by several parameters such as cutting power/speed ratio, material thickness, material composition, gas type, and pressure (Yilbas *et al*., 2014). It is further explained that the Nd: YAG laser

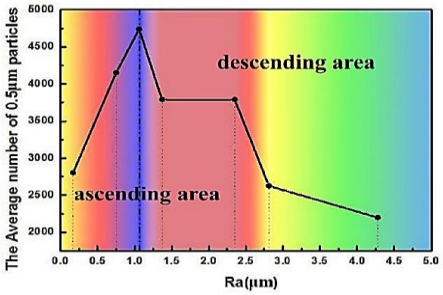

Figure 3. The change of the particle number with the increase of roughness (Chen *et al*., 2019)

Table 2. Specification CO_2 laser (Bharatish *et al*., 2017)

Model	Trumph Laser
Wavelength	10.6 μm
Power	1800-12,000 W
Working distance	500 mm
Field size	2000×1500 mm^2
Beam diameter	0.25 mm

machining process on alumina materials shows that intensity, pulse duration, frequency, and the combined effect of pulse frequency and duration have a significant contribution in determining the surface roughness value (Mohammed *et al*., 2019). The amount of energy and laser absorption also determines the roughness value of alumina ceramics. Experimental results have shown that when lasers are used on alumina, the critical value of roughness is 4.28 μm, as shown in Figure 3.

As can be seen from the graph in Figure 4, cutting speed, gas pressure, and gas composition significantly affect the surface roughness of the material (Umer *et al*., 2017). It is further explained that the 2000-3000mm/min speed produces a better surface finish, but if the speed exceeds 3000mm/min, the surface roughness would be higher. This also applies to gas pressure. The cutting surface will also be smooth when the gas pressure is high. From several descriptions related to surface roughness, many parameters determine the roughness value of the laser process. However, from several references related to surface roughness, only some reports still describe this case, so further studies need to be carried out.

Kerf Width

In the laser beam machining process, kerfs are slots formed during cutting. Thicknesses are usually narrower at the bottom of the sheet specimen than at the top (Dowden, 2017). The kerf width is the distance between the two cutting surfaces separated

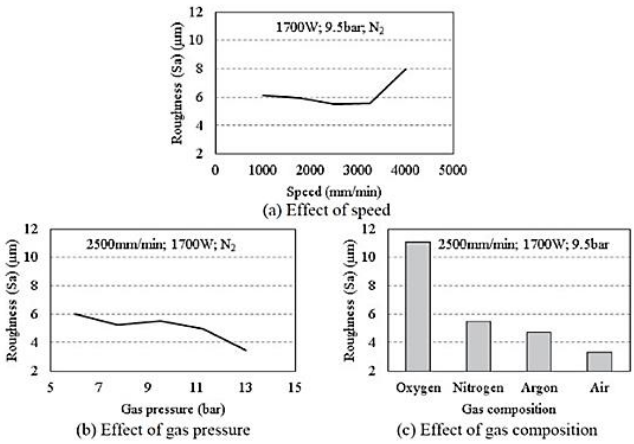

Figure 4. Effect of laser process parameters on the surface roughness (Ra) of the cut surface (Marimuthu *et al.*, 2019a)

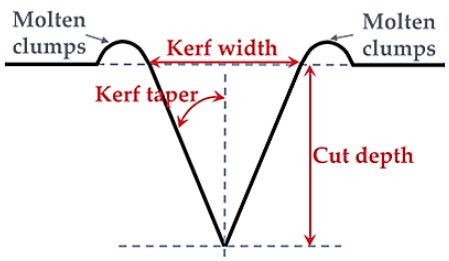

Figure 5. Illustrate the kerf width on cutting (Beausoleil et al., 2020)

by the cutting gap. Two types of kerf widths are obtained during the process where the one on the top (in) side of the kerf is referred to as the top kerf width, and the other is the bottom kerf width on the bottom (out) side of the kerf. cutting depends on focal point size, laser power, sheet material type and thickness, auxiliary gas type and pressure, safety clearance, and cutting speed. Kerf deviation and kerf taper represent the dimensional accuracy of the cut kerf, and these are the calculated attributes. The deviation along the cut is known as kerf deviation, and the angle between the cutting surfaces is known as taper (Sharma and Yadava, 2018). The kerf width of the cut is an important part of the quality process, where a low kerf width is always desirable to get a uniform shape (Mohamad *et al.*, 2020). Based on previous notes, it has been stated that the laser beam machining reacts chemically with the workpiece during the cutting process, which causes the kerf width to follow the diameter size of the beam (Rakshit and Das, 2019). Furthermore, (Ghany and Rafea, 2006) investigated the effect of different pressures of oxygen, nitrogen, or air as an auxiliary gas on cutting quality using CW and pulse laser beam modes by applying different laser powers (up to 1000 W) and cutting speeds (up to 6 m/min). They found that the kerf width decreased with increasing speed, and the minimum kerf width was found using nitrogen. The results were consistent with reports stating that as speed increases, the kerf width decreases and gradually converges to a minimum (Sivaraosa *et al.*, 2014; Beausoleil *et al.*, 2020). An illustration of the kerf width size is shown in Figure 5. From these studies, it is said that gas pressure, type of assist gas, speed, and depth of cut significantly affect the width of the kerf, which may still require an in-depth study of which parameter is the most dominant.

Heat-Affected Zone

HAZ is an unavoidable heat treatment area in the base metal next to the fusion zone, where structural transformation happens during welding (Niv, Tekniska and Skolan, 2015).

Technique for measuring HAZ is shown in Figure 6. Kuar *et al.* (Biswas *et al.*, 2010) investigated Nd: YAG laser microdrilling of alumina to produce a microdrill of higher quality. Lamp current, pulse frequency, air pressure, and pulse width are independent process variables, whereas hole taper and HAZ width are output variables. During laser drilling, thermal expansion residual stresses increase around the heat affected zone. During laser drilling, excessive thermal residual stresses arise around the heat-affected zone due to differences in cooling rates and heat contraction between the outside and internal areas (Yilbas *et al.*, 2011). Measurements are performed around the heat-affected zone, where thermal expansion residual stresses develop. Under specific settings of CW laser cutting, it has been discovered that the HAZ can be lowered by increasing the gas

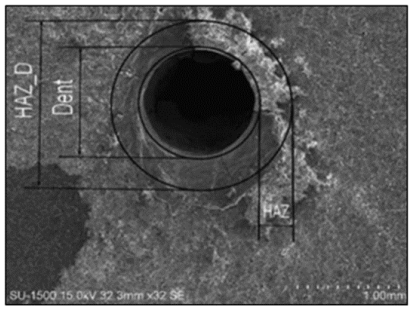

Figure 6. Measurement of the Heat affected zone (Bharatish et al., 2017)

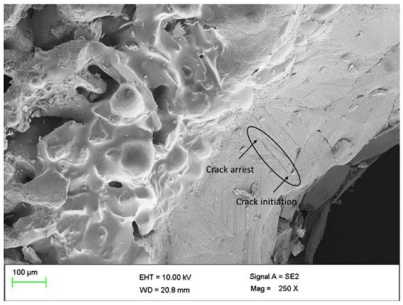

Figure 7. Initial Microcrack in the area of the Heat affected zone (Bharatish et al., 2015)

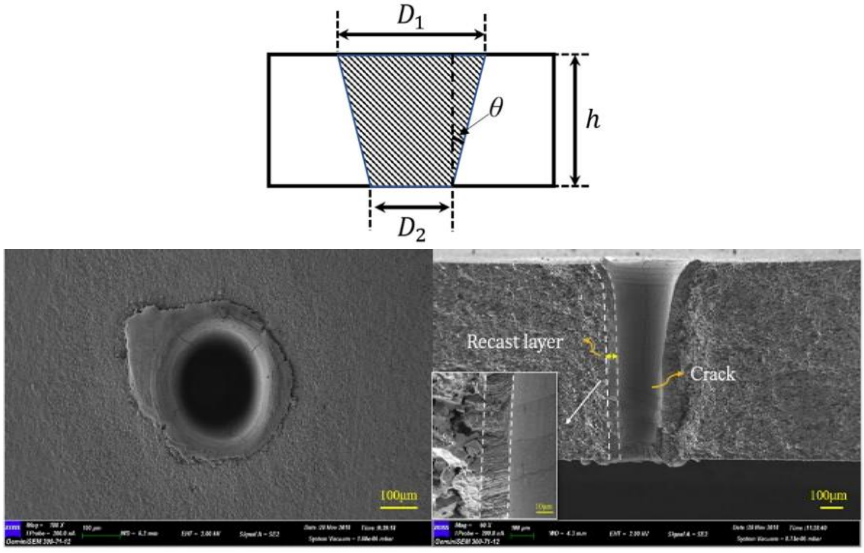

Figure 8. Illustration and SEM Image of the Taper angle (Jia et al., 2020)

pressure, resulting in improved surface quality. This is because the low heat-affected zone is accompanied by a regular and thin oxide layer (Marimuthu *et al*., 2019a). As shown in Figure 7, the action of HAZ can also cause microcracks. Microcrack identity arises in the HAZ region due to high scanning speed and laser power. Reducing scanning speed results in high compressive cyclic residual stresses in the HAZ, causing more damage (Bharatish *et al*., 2015). Heat-affected zones cannot be avoided, as these hot zones can cause microcracks. However, several parameters, such as gas pressure, can reduce the size of HAZ.

Taper Angle

The taper angle is the cylindricity of a hole, with the ideal taper angle corresponding to a perpendicular cylindrical hole. The laser beam's convergent-divergent feature leads to a varied hole diameter as it penetrates deep. According to some findings, the slope of the bore is significantly affected by the pulse energy, the number of pulses, and the beam focus setting (Nandi and Kuar, 2015). Figure 8 displays SEM pictures to illustrate the taper angle and side position. At a fixed peak power of 400 watts and a 10% duty cycle, the report shows a decreasing trend of taper angle and crack with an increase in frequency over 500 Hz (Jia *et al*., 2020). In addition, a single energy pulse supplied that is lowered from millisecond pulses will decrease the energy absorbed by the inner wall of the hole, causing more laser energy to accumulate at the bottom of the hole. In another investigation, as peak power increased, the taper angle reduced (Kacar *et al*., 2009). This demonstrates that the output hole has a larger diameter than the inlet hole. Melt erosion of the pit's sidewall, caused by high vapor above the material's surface during laser irradiation, will force the melt out of research indicates that the width of the hole hole (Tunna *et al*., 2005). Additional research indicates that the width of the hole expands with increased laser power due to the

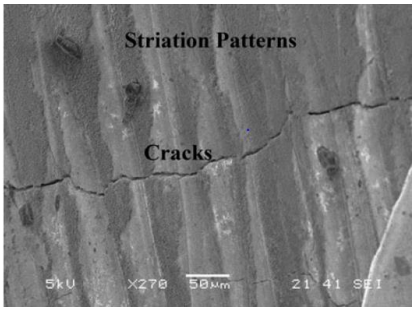

(a)

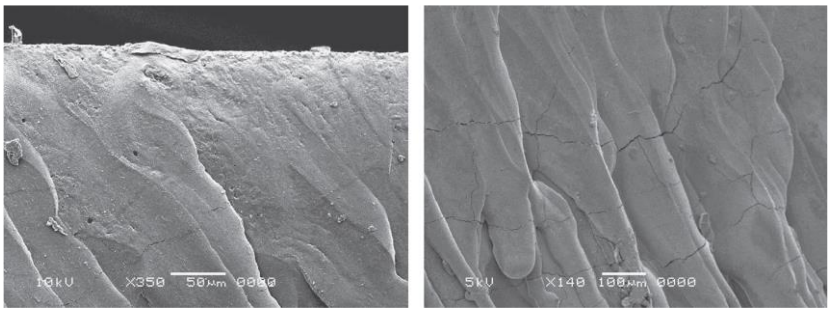

(b)

Figure 9. SEM micrographs of kerf surface: (a) Top surface and (b) The central region of kerf surface (Yilbas *et al*., 2016)

accumulation of heat energy at higher peak power and absorption, resulting in more significant erosion close to the entrance of the pit (Bharatish *et al*., 2013). Exposure as a result of the taper angle is still an interesting discussion, where many parameters such as frequency and power still dominate the size of the taper angle. However, the laser power associated with the increase in temperature still needs to be investigated.

Thermal Crack of Alumina

The laser ablation technique causes numerous issues with alumina degradation because of its high temperature. However, the quality of the cut is still based on the number of cracks on the cut surface, which reduces scanning speed while increasing laser power. Furthermore therefore, this produces a substantial amount of heat corrosion on the cutting surfaces. As shown in Figure 9, the kerf entry and fracture formation were as follows. Cracks had developed on the kerf's surface, a condition often associated with rapid cooling (Yilbas *et al*., 2016). When alumina was sliced, surface fractures were seen.

This condition develops due to significant thermal stress in the shear zone due to the high-temperature gradient (Yilbas et al., 2017). Heat-cracking flaws were eliminated from the cutting results by lowering the cutting speed and laser output power during CO_2 laser machining of Al_2O_3 material with a thickness of 5 mm. Figure 10, displays the results of SEM microscopy, which indicated a ridge on the blade caused by melt instability and the effect of the gas jet on the flow on the surface of the kerf. In addition, microcracks were observed on the machined surface, but they were shallow and did not impact the part's thickness (Qiu *et al*., 2020).

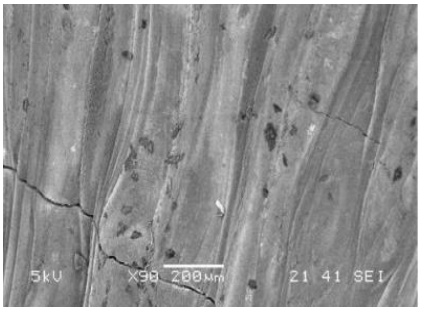

Figure 10. SEM micrographs of laser cut kerf surfaces alumina with laser power of 1500 W and cutting speed of 0.07 m/s (Yilbas *et al*., 2017)

Microcracks in hard and brittle materials are still thought to be caused by cooling gradients or high temperatures (Gautam and Pandey, 2018). A casting layer is created on the machined surface, and considerable thermal stress is present (Yilbas *et al.*, 2017). The cutting of Alumina with a fiber

laser has been experimentally and numerically explored. The results indicate that crack-free cutting may be done with high laser peak power, short pulse duration, and low pulse repetition rate. Due to the change from compressive to tensile stress in a given laser cutting parameter, it has been demonstrated that the no-cracking parameter's threshold can be determined (Yan *et al*., 2011a). From the points above, it can be observed that the formation of cracks is still a big problem in machining alumina, as it has been reported that cracks occurred starting from micro-cracks caused by high thermal effect (Yan *et al*., 2011b). Deeply fractured alumina is caused by very high-temperature gradients and internal stress by thermal shock effects (Panda *et al*., 2002; Barnes, Shrotriya, and Molian, 2007; Li *et al*., 2021). The heat build-up due to repeated laser pulses causes these cracks to continue to expand into multiple melting paths (Zheng *et al*., 2019). Microscopically it has been shown that crack propagation is due to increased heat flux and temperature difference. Apart from that, the thermal stress intensity factor accelerates the occurrence of unstable cracks (Li *et al*., 2021). Furthermore, under different conditions, increasing laser power can reduce thermal crack propagation (Cheng *et al*., 2019; Zheng *et al*., 2019). This is because laser power can penetrate the boundaries of the material causing the melt to pass through the workpiece area. From the perspective of several previous studies, an opinion can be drawn that the effect of high thermal loads is dominant in cracking, where the high temperature is certainly caused by the power density of the laser process.

Effect of Laser Parameters on The Quality of The Alumina Workpiece

Changing laser machining parameters can have a variety of implications, making it exciting to examine the output and quality of alumina materials. The results of observations have been compiled in recent years, and Table 3 input and output parameter values can be a reference point for future research.

1. Impact of Parameter Nd: YAG Laser

1.1. Peak Power

In Nd: YAG Laser Alumina Reducing the Peak Power and Pulse Width parameters affects the average rise in crater diameter, with peak power increasing as pulse duration increases (Kacar *et al*., 2009). In addition, it has been demonstrated that when the peak power increases, the negative taper angle value indicates that the output diameter is larger than the input diameter. Due to increased heat input, the kerf width increases as the peak pulse power increases.

At the lowest peak pulse power, the experimental and simulated pulse widths range by around 40%. This is related to the change in the energy absorption coefficient at various laser powers (Fu *et al*., 2015). This state is caused by high vapor pressure and molten erosion, changing the hole geometry.

1.2. Pulse Frequency

Laser energy is highly dependent on pulse frequency as the effect of this parameter is related to the heat-affected zone (HAZ). When laser machining is in progress, HAZ values should always be avoided, especially for the quality of holes made of alumina materials. The study carried out (Nandi and Kuar, 2015), found that at low pulse frequency, the ability of the laser beam to penetrate deeper into the material was excellent. The presence of air helps to reduce the temperature during the formation of the drilled hole, thereby dissipating the heat and resulting in lessening the formation of HAZ. However, at the mid-beam value, relatively high energy was applied with less time between pulses, which made the HAZ thickness value larger. It was further explained that the thermally affected layer and microcracks increase with increasing pulse energy and feed rate but decrease slightly as pulse frequency increases within the specified range (Zhang *et al*., 1996). Because the flexural strength of the workpiece material is reduced due to the thick heat-affected layer and cracks on the inside, the relationship between pulse energy and pulse frequency becomes dominant in microcracks.

2. Impact of Parameter Fiber Laser

2.1. Laser Power

Laser power is one of the most significant parameters affecting laser fiber on alumina. The influence of this parameter is kerf width, where kerf width is a component of laser process surface quality. The cutting width remains constant at 140 µm while the laser power is between 1400W and 1700W, and it decreases when the laser power is more significant than 1700W (Marimuthu *et al*., 2019a). In addition, the influence of laser power on the taper angle is highly influential, where the value of the taper angle is less when the laser power is 450 W and 475 W than when the laser power is higher (Ghosal and Manna, 2013). The increased laser power on the ceramic.

inlet surface produces a correspondingly higher kerf width. In addition, extremely obvious microcracks and holes are observed during the cutting process (Li *et al*., 2022). There is no doubt that the laser power's power density affects temperature, and one of the reasons for damage to brittle materials is temperature variation. However, this is still under investigation.

Table 3. Summary of parameters with different laser processes

Laser Process	Material Thickness	Laser Parameter	Output Parameter	Observation
Nd: YAG laser (Umer, Mohammed, and Al-Ahmari, 2017)	Al_2O_3 10 mm	Intensity =85-95(%) Frequency=4-8(kHz) Pulse duration=2-6 (µs) Overlap = 33-66(%)	• DL • Surface roughness • MRR	• Intensity and pulse overlap significantly to increase DL • Frequency and pulse duration contribute greatly to RA • Intensity has a significant effect on the increase in MRR
Nd: YAG laser (Nandi and Kuar, 2015)	Al_2O_3 1 mm	Lamp current(l)=20-24 amp Pulse frequency (f)=1-5 kHz Air pressure(p)=0,6-2,2 kg/cm^2 Pulse width(w)=2-18%	• HAZ Thickness • Taper	• I and W effect significant to increase HAZ • I and F significant to increase taper
Nd: YAG laser (Harimkar and Dahotre, 2009)	Al_2O_3 25 mm	Linear scan speed = 100cm/min Laser fluency= 458–687J/cm^2 Pass overlap= <15% of	• Surface roughness • Surface compaction	• Surface compaction decreases with increasing laser fluency • RA decreases with decreasing laser fluency
Nd: YAG laser (Kacar *et al.*, 2009)	Al_2O_3 10 mm	Wavelength= 1064 µm Average power= 600 W Pulse repetition rate= 500 Hz Pulse duration= 2-4 ms Peak power=2,5-5 w	• Average Hole diameter • Average crater diameter • Average taper angle	• Peak power and pulse duration effect to increase crater diameter and hole diameter • The average taper angles decrease because of the increased peak power
Fiber laser (Yan, Li, Sezer, Whitehead, *et al*., 2011b)	Al_2O_3 2 mm and Al MMC (2mm)	Speed = 1000-4000 (mm/min) Laser Power =1400-2000 (W) Gas pressure = 6-13 (bar)	• Oxide layer thickness • HAZ • Surface roughness • Kerf width	• Gas pressure and speed decrease Oxide Layer thickness • Gas pressure effect decreases kerf width • Gas pressure and speed decrease HAZ • The speed increases the RA but gas pressure decreases the RA
Fiber laser (Parmar *et al.*, 2019)	Ti6Al4V3 (3mm) mmSS316 (3 mm)	Laser Power=100-400 (W) Cutting velocity=75-800 mm/min Line energy (J/mm)	• Material separation • Kerf width • HAZ	• Laser power significant to increase material separation, kerf width and HAZ
Fiber laser (Yan, Li, Sezer, Whitehead, *et al*., 2011b)	Al_2O_3 6 mm	Peak power= 600, 800, 1000W Pulse duration=5, 10, 20 ms Pulse repetition rate= 10,20, 50 Hz Feed rate= 0.5, 1, 1.5 (mm/s)	• HAZ • Crack	• High Peak power can decrease HAZ • Peak power and feed rate increases the crack
Fiber laser (Ghosal and Manna, 2013)	Al/Al2O3-MMC 5 mm	Laser power = 400, 500, 700,900, 1000 (W) frequency= 600, 700, 800, 900, 1000 (Hz) Gas pressure= 15,16,17, 18, 20 (bar) Wait time= 0.1, 0.15, 0.2, 0.25, 0.3 (s) Pulse width= 75, 80, 90, 95, 100 (%)	• MRR • Taper	• Power laser and Gas Pressure increase are more dominant in increase of MRR • Frequency and gas pressure significant decrease taper
CO_2 Laser (Yilbas *et al.*, 2011)	Al_2O_3 Coating Al 6065 4 mm	Peak Power = 2000 W Frequency= 100 Hz Duty Cycle = 35 % N2 pressure = 600 (kPa)	• Morphological changes • The metallurgy changes • Micro Crack	• The surface temperature rises rapidly above the melting point of the substrate material. • SEM micrographs show that there are numerous scattered microcracks on the surface.
CO_2 Laser (Yan *et al.*, 2012)	Al_2O_3 4.4 mm	Peak power, P = 350 ≤ P ≤ 3500 (W) Pulse repetition rate, f =10 ≤ f ≤ 500 (Hz) Pulse duty cycle, D=5 ≤ D ≤ 100(%) Pulse duration, ton =0.3 ≤ t_{on} ≤ 100 (ms) Pulse energy, E =1.05 ≤ E ≤ 350 (J)	• Spatter deposition • Hole diameter	• Spatter deposition increased when peak power increased • Spatter deposition increased when peak power decreased • Hole diameter decreased when pulse repetition increased
CO_2 Laser (Yan, Li, Sezer, Wang, Whitehead, *et al.*, 2011a)	Al_2O_3 8 mm	Power= 60 W speed = 10 mm/s 4 scanning cycles	• HAZ • Crack	• Haz and crack increase with decreased power and speed.
CO_2 Laser (Barnes, Shrotriya and Molian, 2007)	Al_2O_3 0.5 mm	Power =100, 150, 200, 250, 300(W) Feed rates =42.3-127 (mm/s)	• Surface fracture • Crack	• Crack and Fracture can decrease with decreased Power and feed rates

2.2. Gas Pressure

The gas pressure parameter is mainly used in the fiber laser process for alumina cutting because it relates to the high heat transfer coefficient and the machining quality. According to a study, increasing the gas's pressure decreases the medium's temperature. The investigation revealed that gas velocity and composition changes contributed to a widespread HAZ trend (Marimuthu *et al*., 2019a). In another investigation, it was revealed that gas pressure significantly affects the quality and escape rate of materials, with a small value of taper being observed at low gas pressure, with the minimum occurring between 18 and 20 Bar of nitrogen gas pressure (Ghosal and Manna, 2013). At low gas pressure, multiple networks of cracks are discernible, while perpendicular striations of the glass phase cover the ceramic with a thickness of several microns (Adelmann and Hellmann, 2013). However, the influence of gas pressure must also be investigated in greater depth, particularly in connection to gas pressure, also referred to as a component of the cracking problem.

3. Impact of Parameter CO_2 Laser

3.1. Laser Power

In the CO_2 laser process, the laser power parameter is generally employed as the primary quality-affecting parameter. One of the advantages of the CO_2 laser is that it has significantly higher power than other laser processes. Studies involving laser power (Bharatish *et al*., 2013; Bharatish *et al*., 2017), show that laser power and drilling time affect the taper. Raising the laser power causes the entrance's diameter to expand, and this is due to the increased reflectivity of the alumina filament in the hole's wall. However, peak power is also connected to laser power, as it has been demonstrated that the greater the hole and residue diameters, the higher the peak power (Bharatish *et al*., 2017). The resulting research demonstrated that as laser power increases, microcracks on the fracture surface grow in size due to excessive tensile stress (Biswas *et al*., 2008). Increasing the laser's output power causes high levels of thermal erosion at the kerf intake and the creation of large cracks leading to the kerf exit in different sessions (Yilbas *et al*., 2016).

3.2. Pulse Frequency

According to previous research, the CO_2 laser's pulse frequency significantly impacts the inlet and outlet circulation. The study found that an increase in pulse frequency affects the value of the entrance and reduces hole circulation (Bharatish *et al*., 2017) This condition is proportional to the stoma periodicity because as the pulse frequency increases, so does the stoma periodicity. This occurs because an increase in pulse frequency reduces peak power intensity, decreasing as the laser beam approaches the exit hole.

Conclusion, Challenges, and Future Directions

Laser machining is the most effective method for cutting alumina ceramics. In addition to becoming suitable for hard and brittle materials such as alumina, the high-temperature ablation method reduces the machining costs associated with cutting time and cutting tools. By a series of tests and simulations, the performance of lasers such as Nd: YAG, fibre lasers, and CO_2 lasers on AL_2O_3 materials has been demonstrated. Each laser has advantages. This article has also covered various types of laser processes associated with laser machining parameters. There are numerous affecting parameters, including pulse duration, frequency, laser power, gas pressure, pulse energy, and cutting speed, with HAZ, surface roughness, taper, microcracks, different of hole diameter, and kerf width serving as independent variables. Some of these circumstances continue to generate cracks and microcracks.

Extreme temperature fluctuations are a common cause of these cracks. As demonstrated in Table 3, several cracks are still dominated by laser power and feed rate influence. Temperature is one of the parameters that affect the cracking problem in alumina. In contrast, the temperature is determined by the high and low laser power, as defined by the extent to which the effect of laser power reacts to the number and length of cracks in alumina ceramic. According to some studies, high laser power results in a small number of cracks; nevertheless, under various conditions, high laser power also creates more significant cracks. Compared to other lasers, such as fiber and Nd: YAG, CO_2 lasers offer an extremely high output of power; In addition, the CO_2 laser has a wavelength of 10.6m, which makes it suitable for large-scale cutting.

Acknowledgment

The author would like to thank Universiti Teknikal Malaysia Melaka for providing a source of funds to conduct research with the INDUSTRI (IRMG) / RSADVANCED / 2020 / FKP-COSSID / I00041 grant number.

References

Abdullah, L., Jamaludin, Z., Chiew, T.H., Rafan, N.A., and Shaaban, A. (2013). Spectral Analysis of Cutting Forces Data for XY Table Ballscrew Drive System. In Applied Mechanics and Materials, 471:241-246. https://doi.org/10.4028/www.scientific.net/amm.471.241

Abdullah, L., Jamaludin, Z., Maslan, M.N., Jamaludin, J., Halim, I., Rafan, N.A., and Chiew, T.H. (2015). Assessment on Tracking Performance of Cascade P/PI, NPID and NCasFF Controller for Precise Positioning of XY Table Ballscrew Drive System, Procedia CIRP, 26:212-216. https://doi.org/10.1016/j.procir.2014.07.111

Adelmann, B., and Hellmann, R. (2013). Investigation on flexural strength during fiber laser cutting of alumina. Physics Procedia, 41:405-407. https://doi.org/10.1016/j.phpro.2013.03.094

Arshad, A., Yajid, M.A.M., and Idris, M.H. (2020). 'Laser Glazed Lanthanum Zirconate Thermal Barrier Coating', (12806), pp. 12,806-12,811.

Barnes, C., Shrotriya, P., and Molian, P. (2007). Water-assisted laser thermal shock machining of alumina. International Journal of Machine Tools and Manufacture, 47(12-13):1,864-1,874. https://doi.org/10.1016/j.ijmachtools.2007.04.003

Beausoleil, C. Sarvestani, H.Y., Katz, Z., Gholipour, J., and Ashraf, B. (2020). Deep and high precision cutting of alumina ceramics by picosecond laser, Ceramics International, 46(10):15,285-15,296. https://doi.org/10.1016/j.ceramint.2020.03.069

Bharatish, A., Murthy, H.N.N., Anand, B., Madhusoodana, C.D., Praveena, G.S., and Krishna, M. (2013). Optics & Laser Technology Characterization of hole circularity and heat affected zone in pulsed CO_2 laser drilling of alumina ceramics, Optics and Laser Technology, 53:22-32. https://doi.org/10.1016/j.optlastec.2013.04.010

Bharatish, A., Murthy, H.N.N., Anand, B., Satyanarayana, B.S., and M. Krishn, M. (2015). Optics & Laser Technology Evaluation of thermal residual stresses in laser drilled alumina ceramics using Micro-Raman spectroscopy and COMSOL Multiphysics, Optics and Laser Technology, 70:76-84. https://doi.org/10.1016/j.optlastec.2015.01.009

Bharatish, A., Murthy, H.N.N., Anand, B., Subramanya, K.N., Krishna, M., and Srihari, P.V. (2017). Assessment of drilling characteristics of alumina coated on aluminium using CO_2 laser, Measurement: Journal of the International Measurement Confederation, 100:164-175. https://doi.org/10.1016/j.measurement.2016.12.059

Bhattacharyya, B., and Doloi, B. (2020). Machining processes utilizing thermal energy, Editor(s): Bijoy Bhattacharyya, Biswanath Doloi, Modern Machining Technology, Academic Press, P. 161-363. https://doi.org/10.1016/B978-0-12-812894-7.00004-9

Biswas, R. Kuar, A.S., Sarkar, S., and Mitra, S. (2010). Optics & Laser Technology A parametric study of pulsed Nd : YAG laser micro-drilling of gamma-titanium aluminide. Optics and Laser Technology, 42(1):23-31. https://doi.org/10.1016/j.optlastec.2009.04.011

Biswas, R., Kuar, A.S., and Mitra, S. (2008). Influence of machining parameters on surface roughness in Nd : YAG laser micro-cutting of alumina-aluminium interpenetrating phase composite Influence of machining parameters on surface roughness in Nd : YAG laser micro-cutting of alumina - aluminium interpenetrating phase composite', 2(3-4):252-264 https://doi.org/10.1504/IJSURFSE.2008.020497

Black, I., and Chua, K.L. (1997). Laser cutting ceramic tile. Optics & Laser Technology, 29(4):193-205. https://doi.org/10.1016/S0030-3992(97)00005-4

Carvalho, A., Cangueirod, L., Oliveirad, V., Vilard, R., Fernandes, M.H., and Monteiro, F.J. (2018). Femtosecond laser microstructured Alumina toughened Zirconia: A new strategy to improve osteogenic differentiation of hMSCs. Applied Surface Science, 435:1,237-1,245. https://doi.org/10.1016/j.apsusc.2017.11.206

Carvalho, A., Grenho, L., Fernandes, M.H., Daskalova, A., Trifonov, A., Buchvarov, I., and Monteiro, F.J. (2020). Femtosecond laser microstructuring of alumina toughened zirconia for surface functionalization of dental implants. Ceramics International, 46(2):1,383-1,389. https://doi.org/10.1016/j.ceramint.2019.09.101

Chen, J.X., Qina, J.B., Lua, L.H., Lia, H.Y., Miaob, X.X., Niub, L.F., Liub, H., Zhoub, G.R., Yaob, C.Z., Yuanb, X.D., and Pen, H.M. (2019). Study on laser-stricken damage to alumina ceramic layer of different surface roughness. Results in Physics, 15:102723 https://doi.org/10.1016/j.rinp.2019.102723

Cheng, X., Yang, L., Wang, M., Cai, Y., Wang, Y., and Ren, Z. (2019). Laser beam induced thermal-crack propagation for asymmetric linear cutting of silicon wafer. Optics and Laser Technology, 120(August):105765. https://doi.org/10.1016/j.optlastec.2019.105765

Dowden, J. (2017). Springer Series in Materials Science 119 The Theory of Laser Materials Processing. second edi. Edited by J. Dowden *et al*. 2nd edition: © Springer International Publishing AG 2017. https://doi.org/10.1007/978-3-319-56711-2

Dubey, A.K., and Yadava, V. (2008). Laser beam machining-A review. International Journal of Machine Tools and Manufacture., 48(6):609-628. https://doi.org/10.1016/j.ijmachtools.2007.10.017

Fu, C.H., Sealya, M.P., Guoa Y.B., and Wei, X.T. (2015). Finite element simulation and experimental validation of pulsed laser cutting of nitinol. Journal of Manufacturing Processes, 19:81-86. https://doi.org/10.1016/j.jmapro.2015.06.005

Furukawa, G.T., Douglas, T.B., McCoske, R.E., and Ginnings, D.C. (1956). Thermal Properties of Aluminum Oxide From Z), 57(2). https://doi.org/10.6028/jres.057.008

Gautam, G.D., and Pandey, A.K. (2018a). Pulsed Nd : YAG laser beam drilling : A review. Optics and Laser Technology. Elsevier Ltd, 100, pp. 183-215. https://doi.org/10.1016/j.optlastec.2017.09.054

Gautam, G.D., and Pandey, A.K. (2018b). Pulsed Nd: YAG laser beam drilling: A review. Optics and Laser Technology. 100:183-215. https://doi.org/10.1016/j.optlastec.2017.09.054

Ghany, K.A., and Rafea, H.A. (2006). Using an Nd: YAG laser and six axes robot to cut zinc-coated steel. Int. J. Adv. Manuf. Technol., 28:1,111-1,117. https://doi.org/10.1007/s00170-004-2468-x

Ghosal, A., and Manna, A. (2013). Optics & Laser Technology Response surface method-based optimization of ytterbium fiber laser parameter during machining of Al / Al2O3 - MMC. Optics and Laser Technology, 46:67-76. https://doi.org/10.1016/j.optlastec.2012.04.030

Harimkar, S.P., and Dahotre, N.B. (2009). Rapid surface microstructuring of porous alumina ceramic using continuous wave Nd: YAG lase. Journal of Materials Processing Technology, 209(10):4,744-4,749. https://doi.org/10.1016/j.jmatprotec.2008.12.001

Jia, X. Chen, Y., Wang, H., Zhu, G., and Zhu, X. (2020). Experimental study on nanosecond-millisecond combined pulse laser drilling of alumina ceramic with di ff erent spot sizes. Optics and Laser Technology, 130(November 2019):106,351. https://doi.org/10.1016/j.optlastec.2020.106351

Kacar, E. Mutlua, M., Akmana, E., Demira, A., Candana, L., Canela, T., Gunayd, V., and Sınmazcelik, T. (2009). Characterization of the drilling alumina ceramic using Nd: YAG pulsed laser. Journal of Materials Processing Technology, 209(4):2,008-2,014. https://doi.org/10.1016/j.jmatprotec.2008.04.049

Khed, R. (2015). Experimental Investigation and Analysis of Process Parameters in Laser Beam Machining of Aluminium Alloy 8011., 4(9):326-333. https://doi.org/10.17577/IJERTV4IS090359

Li, M., Han, H., Jiang, X., Zhang, X., and Chen, Y. (2022). Surface morphology and defect characterization during high-power fiber laser cutting of SiC particles reinforced aluminum metal matrix composite. Optics and Laser Technology. Elsevier Ltd., 155(June):108419. https://doi.org/10.1016/j.optlastec.2022.108419

Li, Y. Hub, Y., Congb, W., Zhia, L., and Guoa, Z. (2017). Additive manufacturing of alumina using laser engineered net shaping: Effects of deposition variables. Ceramics International, 43(10):7,768-7,775. https://doi.org/10.1016/j.ceramint.2017.03.085

Li, Y., Li, Q., Wu, X., Shao, Y., Li, L., and Song, F. (2021). Cracking in the translucent alumina ceramic during flame thermal shock. Ceramics International, 47(21):30,974-30,979. https://doi.org/10.1016/j.ceramint.2021.07.154

Marimuthu, S., Dunleavey, J., and Smith, B. (2019b). Laser Based Machining of Aluminum Metal Matrix Composites. Procedia CIRP, 85:243-248. https://doi.org/10.1016/j.procir.2019.09.007

Marimuthu, S., Dunleavey, J., Liu, Y., Antar, M., and Smith, B. (2019a). Laser cutting of aluminum-alumina metal matrix composite. Optics and Laser Technology, 117(April):251-259. https://doi.org/10.1016/j.optlastec.2019.04.029

Mohamad, W.N.F., Kasim, M.S., Norazlina, M.Y., Hafiz, M.S.A., Izamshah, R., and Mohamed, S.B. (2020). Effect of standoff distance on the kerf characteristic during abrasive water jet machining. Results in Engineering, 6(January):4-8. https://doi.org/10.1016/j.rineng.2020.100101

Mohammed, M.K., Umer, U., and Al-Ahmari, A. (2019). Optimization of Nd: YAG laser for microchannels fabrication in alumina ceramic. Journal of Manufacturing Processes, 41(January):148-158. https://doi.org/10.1016/j.jmapro.2019.03.036

Nagimova, A., and Perveen, A. (2019). ScienceDirect A review on Laser Machining of hard to cut materials. Materials Today: Proceedings, 18:2,440-2,447. https://doi.org/10.1016/j.matpr.2019.07.092

Nandi, S., and Kuar, A.S. (2015). Parametric optimisation of Nd: YAG laser micro-drilling of alumina using NSGA II. International Journal of Machining and Machinability of Materials, 17(1):1-21. https://doi.org/10.1504/IJMMM.2015.069209

Niv, A., Tekniska, K. T.H.K. and Skolan, G. (2015). Welding of dissimilar metals in different welding positions. Available from: www.semanticscholar.org/author/Mimmi-B%C3%A4ck/115963014

Oosterbeek, R.N., Ward, T., Ashforth, S., Bodley, O., Rodda, A. E., and Simpson, M.C. (2016). Fast femtosecond laser ablation for efficient cutting of sintered alumina substrates. Optics and Lasers in Engineering, 84:105-110. https://doi.org/10.1016/j.optlaseng.2016.04.007

Panda, P.K., Kannana, T.S., Duboisb, J., Olagnonb, C., and Fantozzi, G. (2002). Thermal shock and thermal fatigue study of alumina. Journal of the European Ceramic Society, 22(13):2,187-2,196. https://doi.org/10.1016/S0955-2219(02)00022-5

Pappas, J.M., Thakur, A.R., and Dong, X. (2020). Effects of zirconia doping on additively manufactured alumina ceramics by laser direct deposition. Materials & Design, 192:108711. https://doi.org/10.1016/j.matdes.2020.108711

Parmar, V., Kumar, A., Prakasha, G.V., Dattab, S., and Kalyanasundaram, D. (2019). Investigation, modeling and validation of material separation mechanism during fiber laser machining of medical grade titanium alloy Ti6Al4V and stainless steel SS316L. Mechanics of Materials, 137(January):103125. https://doi.org/10.1016/j.mechmat.2019.103125

Qiu, Y. Wua, J.M., Chena, A.N., Chena, P., Yanga, Y., Liu, R. Z., Gong Chena, G., Chena, S., Shia, Y.S. and Lia, C.H. (2020). Balling phenomenon and cracks in alumina ceramics prepared by direct selective laser melting assisted with pressure treatment. Ceramics International, 46(9):13,854-13,861. https://doi.org/10.1016/j.ceramint.2020.02.178

Rakshit, R., and Das, A.K. (2019). A review on cutting of industrial ceramic materials. Precision Engineering, 59(January):90-109. https://doi.org/10.1016/j.precisioneng.2019.05.009

Ruys, A. (2019). 1 - Introduction to alumina ceramics, Editor(s): Andrew Ruys, In Woodhead Publishing Series in Biomaterials, Alumina Ceramics, Woodhead Publishing, P. 1-37. https://doi.org/10.1016/B978-0-08-102442-3.00001-4

Salonitis, K., Stournaras, A., Tsoukantas, G., Stavropoulos, P., and Chryssolouris, G. (2007). A theoretical and experimental investigation on limitations of pulsed laser drilling. Journal of Materials Processing Technology, 183(1):96-103. https://doi.org/10.1016/j.jmatprotec.2006.09.031

Samant, A.N., and Dahotre, N.B. (2008). Computational predictions in single-dimensional laser machining of alumina. International Journal of Machine Tools and Manufacture, 48(12-13):1345-1353. https://doi.org/10.1016/j.ijmachtools.2008.05.004

Samant, A.N., and Dahotre, N.B. (2009). Laser machining of structural ceramics-A review. Journal of the European Ceramic Society, 29(6):969-993. https://doi.org/10.1016/j.jeurceramsoc.2008.11.010

Sarkar, B., Reddy, M.M., and Debnath, S. (2017). Effect of machining parameters on surface finish of Inconel 718 in end milling. MATEC Web of Conferences. Edited by H. L. Yuan *et al*., 95, p. 02009. https://doi.org/10.1051/matecconf/20179502009

Sharma, A., and Yadava, V. (2018). Experimental analysis of Nd-YAG laser cutting of sheet materials - A review. Optics and Laser Technology, 98:264-280. https://doi.org/10.1016/j.optlastec.2017.08.002

Sharma, P., Mishra, D.K., and Dixit, P. (2020). Experimental investigations into alumina ceramic micromachining by Experimental investigations into alumina ceramic process micromachining by electrochemical discharge machining. Procedia Manufacturing, 48(2019):244-250. https://doi.org/10.1016/j.promfg.2020.05.044

Shen, J.Y. Luo, C.B., Zeng, W.M., Xu, X.P., and Gao, Y.S. (2002). Ceramics grinding under the condition of constant pressure. Journal of Materials Processing Technology, 129(1-3):176-181. https://doi.org/10.1016/S0924-0136(02)00636-2

Sivaraosa, Milkeya. K.R., Samsudina, A.R., Dubeyb, A.K., and Kiddc, P. (2014). Comparison between Taguchi Method and Response Surface. Modelling CO_2 Laser Machining, 8(1):35-42.

Tanaka, S., Yamada, S., Soga, R., Komurasaki, K., Kawashima, R., and Koizumi, H. (2019). Alumina reduction by laser ablation using a continuous-wave CO_2 laser toward lunar resource utilization. Vacuum, 167(August 2018):495-499. https://doi.org/10.1016/j.vacuum.2018.07.054

Tuersley, I.P., Jawaid, A., and Pashby, I.R. (1994). Review: Various methods of machining advanced ceramic materials. Journal of Materials Processing Tech., 42(4):377-390. https://doi.org/10.1016/0924-0136(94)90144-9

Tunna, L., O'Neilla, W., Khana, A., and Sutcliffe, C. (2005). Analysis of laser micro drilled holes through aluminium for micro-manufacturing applications, Optics and Lasers in Engineering, 43(9):937-950. https://doi.org/10.1016/j.optlaseng.2004.11.001

Umer, U., Mohammed, M.K., and Al-Ahmari, A. (2017). Multi-response optimization of machining parameters in micro milling of alumina ceramics using Nd: YAG laser. Measurement: Journal of the International Measurement Confederation, 95:181-192. https://doi.org/10.1016/j.measurement.2016.10.004

Wen, Q. Luan, X., Wang, L., Xu, X., Ionescu, E., and Riedel, R. (2019). Journal of the European Ceramic Society Laser ablation behavior of SiHfC-based ceramics prepared from a single-source precursor: Effects of Hf incorporation into SiC. Journal of the European Ceramic Society, 39(6):2,018-2,027. https://doi.org/10.1016/j.jeurceramsoc.2019.01.040

Yan, Y., Ji, L., Bao, Y., and Jiang, Y. (2012). An experimental and numerical study on laser percussion drilling of thick-section alumina. Journal of Materials Processing Technology, 212(6):1,257-1,270. https://doi.org/10.1016/j.jmatprotec.2012.01.010

Yan, Y., Li, L., Sezer, K., Wang, W., and Whitehead, D. (2011a). CO_2 laser underwater machining of deep cavities in alumina. Journal of the European Ceramic Society, (15):2,793-2,807. https://doi.org/10.1016/j.jeurceramsoc.2011.06.015

Yan, Y., Li, L., Sezer, K., Whitehead, D., Ji, L., Bao, Y., and Jiang, Y. (2011b). Experimental and theoretical investigation of fibre laser crack-free cutting of thick-section alumina. International Journal of Machine Tools and Manufacture, 51(12):859-870. https://doi.org/10.1016/j.ijmachtools.2011.08.004

Yilbas, B.S., Akhtar, S.S., and Karatas, C. (2014). Laser cutting of rectangular geometry into alumina tiles. Optics and Lasers in Engineering, 55:35-43. https://doi.org/10.1016/j.optlaseng.2013.10.006

Yilbas, B.S., Akhtar, S.S., and Karatas, C. (2016). Laser machining of different diameter holes in alumina ceramic: Thermal stress analysis. Machining Science and Technology, 20(3):349-367. https://doi.org/10.1080/10910344.2016.1191024

Yilbas, B.S., Karatas, C., Arifa, A.F.M. and Aleem, B.J.A. (2011). Laser control melting of alumina surfaces and thermal stress analysis. Optics and Laser Technology, 43(4):858-865. https://doi.org/10.1016/j.optlastec.2010.10.009

Yilbas, B.S., Shaukat, M.M., and Ashraf, F. (2017). Laser cutting of various materials: Kerf width size analysis and life cycle assessment of cutting process. Optics and Laser Technology, 93:67-73. https://doi.org/10.1016/j.optlastec.2017.02.014

You, K. Yan, G., Luo, X., Gilchrist, M.D., and Fang, F. (2020). Advances in laser assisted machining of hard and brittle materials. Journal of Manufacturing Processes, 58(September 2019):677-692. https://doi.org/10.1016/j.jmapro.2020.08.034

Zhang, J.H., Lee, T.C., Ai, X., and Lau W.S. (1996). Investigation of the surface integrity of laser-cut ceramic. Journal of Materials Processing Technology, 57(3-4):304-310. https://doi.org/10.1016/0924-0136(95)02085-3

Zheng, Y., Zhang, K., Liu, T.T., Liao, W.H., Zhang, C.D., and Shao, H. (2019). Cracks of alumina ceramics by selective laser melting. Ceramics International, 45(1):175-184. https://doi.org/10.1016/j.ceramint.2018.09.149